THE JOURNAL OF BIOLOGICAL CHEMISTRY VOL. 285, NO. 38, pp. 29156–29164, September 17, 2010

Molecular Characterization of *N*-Acetylaspartylglutamate Synthetase[S]

Received for publication, February 6, 2010, and in revised form, July 19, 2010 Published, JBC Papers in Press, July 19, 2010, DOI 10.1074/jbc.M110.111765

Ivonne Becker[1], **Julia Lodder**[1], **Volkmar Gieselmann, and Matthias Eckhardt**[2]

From the Institute of Biochemistry and Molecular Biology, University of Bonn, D-53115 Bonn, Germany

The dipeptide *N*-acetylaspartyl-glutamate (NAAG) is an abundant neuropeptide in the mammalian brain. Despite this fact, its physiological role is poorly understood. NAAG is synthesized by a NAAG synthetase catalyzing the ATP-dependent condensation of *N*-acetylaspartate and glutamate. *In vitro* NAAG synthetase activity has not been described, and the enzyme has not been purified. Using a bioinformatics approach we identified a putative dipeptide synthetase specifically expressed in the nervous system. Expression of the gene, which we named NAAGS (for NAAG synthetase) was sufficient to induce NAAG synthesis in primary astrocytes or CHO-K1 and HEK-293T cells when they coexpressed the NAA transporter NaDC3. Furthermore, coexpression of NAAGS and the recently identified *N*-acetylaspartate (NAA) synthase, Nat8l, in CHO-K1 or HEK-293T cells was sufficient to enable these cells to synthesize NAAG. Identity of the reaction product of NAAGS was confirmed by HPLC and electrospray ionization tandem mass spectrometry (ESI-MS). High expression levels of NAAGS were restricted to the brain, spinal cord, and testis. Taken together our results strongly suggest that the identified gene encodes a NAAG synthetase. Its identification will enable further studies to examine the role of this abundant neuropeptide in the vertebrate nervous system.

N-acetylaspartylglutamate (NAAG)[3] is an abundant neuropeptide in the central nervous system of mammals, present in high micromolar to low millimolar concentrations (for review see Refs. 1–3). It was first identified in rabbit and horse brain tissue by Curatolo *et al.* (4) and in bovine brain by Miyamoto *et al.* (5). NAAG is present in all regions of the central nervous system of mammals, though the highest concentrations are found in the spinal cord and stem brain (6). Despite its abundance throughout the mammalian nervous system, its physiological role is not fully understood.

Because NAAG synthesis in sensory ganglia was not blocked by translation inhibitors, it was assumed that NAAG is not derived from a post-translational process, but is synthesized by a neuron specific NAAG synthetase, catalyzing the condensation of *N*-acetylaspartate (NAA) and glutamate (Ref. 7; see Fig. 1). After its calcium-dependent release from synaptic terminals, NAAG can be degraded by glutamate carboxypeptidase II (*N*-acetylated-α-linked-acidic dipeptidase; GCP-II) or GCP-III, membrane-bound enzymes mainly expressed by astrocytes (for review see Ref. 8). The released NAA is then taken up by glial cells via the high-affinity, sodium-dependent dicarboxylate (NaDC3) transporter (9). In oligodendrocytes, NAA can then be hydrolyzed to aspartate and acetate by aspartoacylase II (8). The released acetate may be used for lipid synthesis by myelinating oligodendrocytes (10, 11). To what extent NAA is taken up by astrocytes *in vivo* and its metabolic fate in these cells is not clear. Deficiency in aspartoacylase II leads to accumulation of NAA, but also NAAG (11), and causes a rare leukodystrophy, Canavan disease (12, 13).

Studies on the role of NAAG mainly relied on increasing NAAG concentrations through inhibition of GCP-II or injecting NAAG. Changes in NAAG concentration affect long-term potentiation and depression in the hippocampus (14, 15). Impaired NAAG-mediated signaling has been implicated in schizophrenia (16, 17). Elevating NAAG levels through GCP-II inhibition is also neuroprotective in different *in vivo* and *in vitro* model systems (see Ref. 16 for review). The effects of NAAG appear to be mediated by its agonistic binding to type 3 metabotropic glutamate receptor (mGluR3). In this model, activation of presynaptic mGluR3 reduces neurotransmitter release, thus reducing glutamate release from glutamatergic synapses. In addition, activation of mGluR3 on astrocytes may be neuroprotective by stimulating TGF-β release (16). However, a recent study suggested that NAAG may not be an agonist of mGluR3 (18). In principle, inhibition of GCP-II may also be neuroprotective by reducing the amount of glutamate released from NAAG.

In Pelizaeus-Merzbacher disease, which is caused by mutations in the proteolipid protein, a major myelin component, elevated NAAG concentrations in the cerebrospinal fluid were observed (19). In addition, increased concentrations of NAAG have been found in Pelizaeus-Merzbacher-like disease, which is caused by mutation in the connexin 47 gene (20) Whether elevated NAAG levels contribute to the pathogenesis of these diseases is currently unknown.

The enzyme(s) synthesizing NAAG have not been characterized. Biosynthesis of NAAG could be demonstrated in neural tissue explants (21–23), astrocytes (23), and in neuroblastoma cells (24). However, no *in vitro* enzyme assay could be established, preventing purification of the enzyme. We hypothesized

[S] The on-line version of this article (available at http://www.jbc.org) contains supplemental Fig. S1 and Table S1.

[1] Both authors contributed equally to this work.

[2] To whom correspondence should be addressed: Institute of Biochemistry and Molecular Biology, University of Bonn, Nussallee 11, 53115 Bonn, Germany. Tel.: 49-228-73-4735; Fax: 49-228-73-2416; E-mail: eckhardt@uni-bonn.de.

[3] The abbreviations used are: NAAG, *N*-acetylaspartylglutamate; ESI-MS, electrospray ionization-mass spectrometry; GCP-II/III, glutamate carboxypeptidase II/III; mGluR3, metabotropic glutamate receptor type 3; NAA, *N*-acetylaspartate; NAAGS, NAAG synthetase; NaDC3, sodium-dependent dicarboxylate transporter 3; RACE, rapid amplification of cDNA ends; ASPA-II, aspartoacylase II.

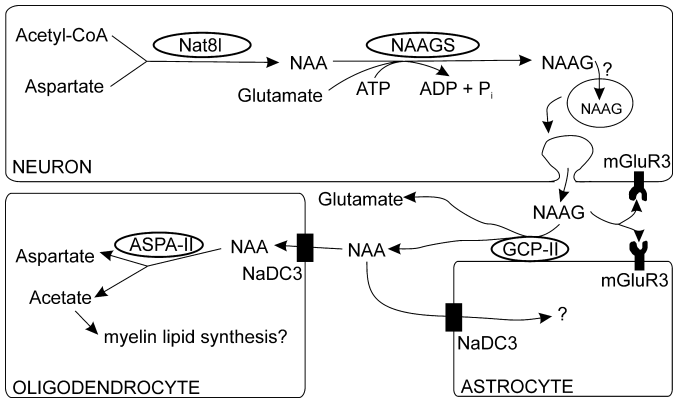

FIGURE 1. **Schematic presentation of NAAG metabolism.** The aspartate *N*-acetyltransferase Nat8l (*NAA synthase*), a membrane-bound microsomal *N*-acetyltransferase, catalyzes the *N*-acetylation of aspartate, forming NAA. The condensation of NAA and glutamate is catalyzed by NAAGS, in an ATP-dependent and ADP-generating reaction. NAAG is released from nerve terminals most likely via synaptic vesicles. The transporter responsible for the translocation of NAAG into synaptic vesicles is unknown. Released NAAG can be degraded extracellularly by GCP-II or GCP-III (not shown), liberating NAA and glutamate. NAAG may also bind to mGluR3 on presynaptic membranes and astrocytes. The NAA transporter NaDC3 is expressed by astrocytes and oligodendrocytes. Using ASPA-II, the latter can hydrolyze NAA. The released acetate may be used for myelin lipid synthesis in myelinating oligodendrocytes (see Ref. 8 for review).

that the NAAG synthetase shall be homologous to other peptide synthetases or amino acid ligases. Using prokaryotic and eukaryotic genes as queries, BLAST searches were performed that identified a putative dipeptide synthetase, NAAGS (for NAAG synthetase), highly expressed in the nervous system. We show here that expression of this gene together with the recently identified NAA synthase is necessary and sufficient to induce NAAG synthesis in CHO-K1 or HEK-293T cells, indicating that the newly identified gene encodes an *N*-acetylaspartylglutamate synthetase.

EXPERIMENTAL PROCEDURES

BLAST Search and Sequence Analysis—Protein sequences of known eukaryotic and prokaryotic peptide synthetases/amino acid ligases were used as queries for BLAST searches of the GenBank™ database via NCBI BLAST. Identified sequences were used to perform additional BLAST searches. Candidate genes were further examined regarding their expression pattern using the NCBI EST database. Candidate genes strongly expressed in nervous tissue were further analyzed by database searches to identify homologous genes in other organisms. Multiple sequence alignments were calculated using M-Coffee (25).

Northern Blotting—Total RNA was isolated from various organs of adult (10-week-old) C57BL/6 mice using Trizol (Sigma) following the manufacturer's instruction. RNAs (20 μg per lane) were separated by gel electrophoresis in 1% agarose/1 M formaldehyde gels and transferred onto Hybond N+ nylon membranes (GE Healthcare Europe, Freiburg, Germany) as described (26). Membranes were hybridized to digoxigenin-labeled antisense NAAGS cRNA probe, followed by chemiluminescence detection, as described (26).

cDNA Synthesis and Real-time RT-PCR—Total RNA from various mouse tissues (of 10-week-old C57BL/6 mice) was prepared using Trizol. Superscript II reverse transcriptase (Invitrogen, Karlsruhe, Germany) and oligo(dT) primer were used to synthesize cDNA, according to the manufacturer's instruction. Quantitative real-time PCR was done using SybrGreen mix (Sigma) and the specific primers shown in supplemental Table S1, as described (27). Ubiquitin C was used

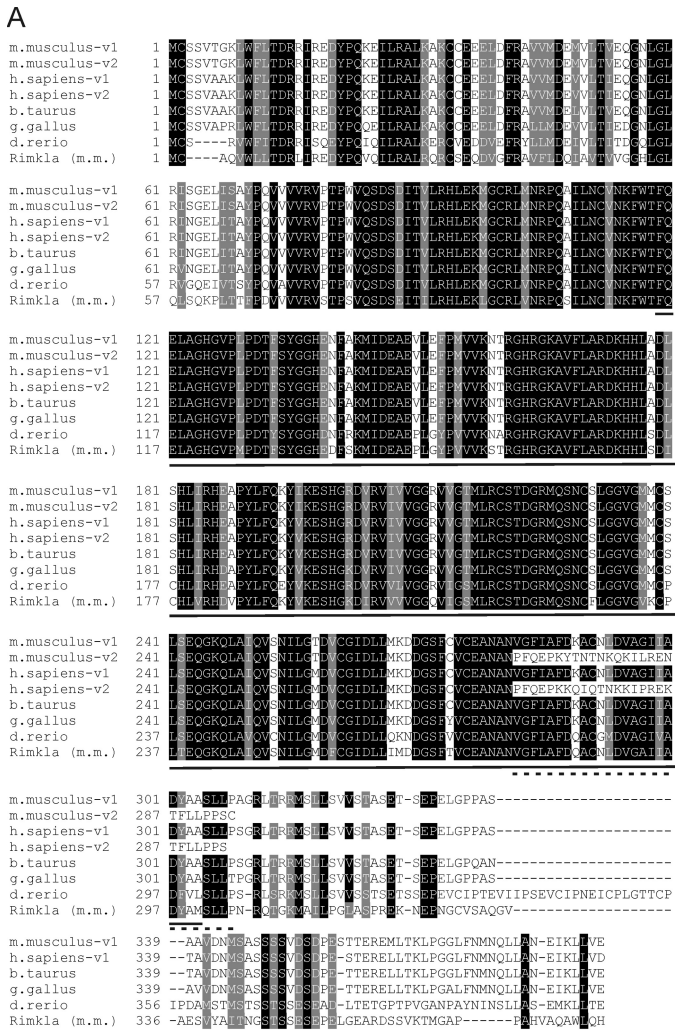

FIGURE 2. **Sequence comparison of NAAG synthetases of different vertebrate species.** *A*, amino acid sequences of NAAG synthetases from mouse (m.musculus; GenBank™ accession number: NP_081940), human (h.sapiens; NP_065785), bovine (b.taurus; NP_001069581), chicken (g.gallus; XP_416481), and zebrafish (d.rerio; NP_001004554) were aligned using the ClustalW algorithm. The sequence of the related mouse Rimkla gene product (Rimkla m.m.; NP_808240) was included in the alignment. The alignment was manually corrected, where residues were obviously misaligned. Both variants of NAAGS (v1, v2) identified in mouse and human are shown. Residues identical in all sequences (including mouse Rimkla) are shaded *black*, and similar residues in all sequences are shaded *gray* (note that the C-terminal part of the splice variants v2, indicated by a *broken line*, was not considered). The ATP-grasp domain is *underlined*. *B*, two NAAGS variants (v1 and v2) are generated by differential polyadenylation and alternative splicing. The internal polyadenylation site (pA) in exon 6 and the polyadenylation site at exon 9 were confirmed by 3′-RACE-PCR (data not shown). The second pA site at exon 6 was deduced from the cDNA sequences in the ensemble database.

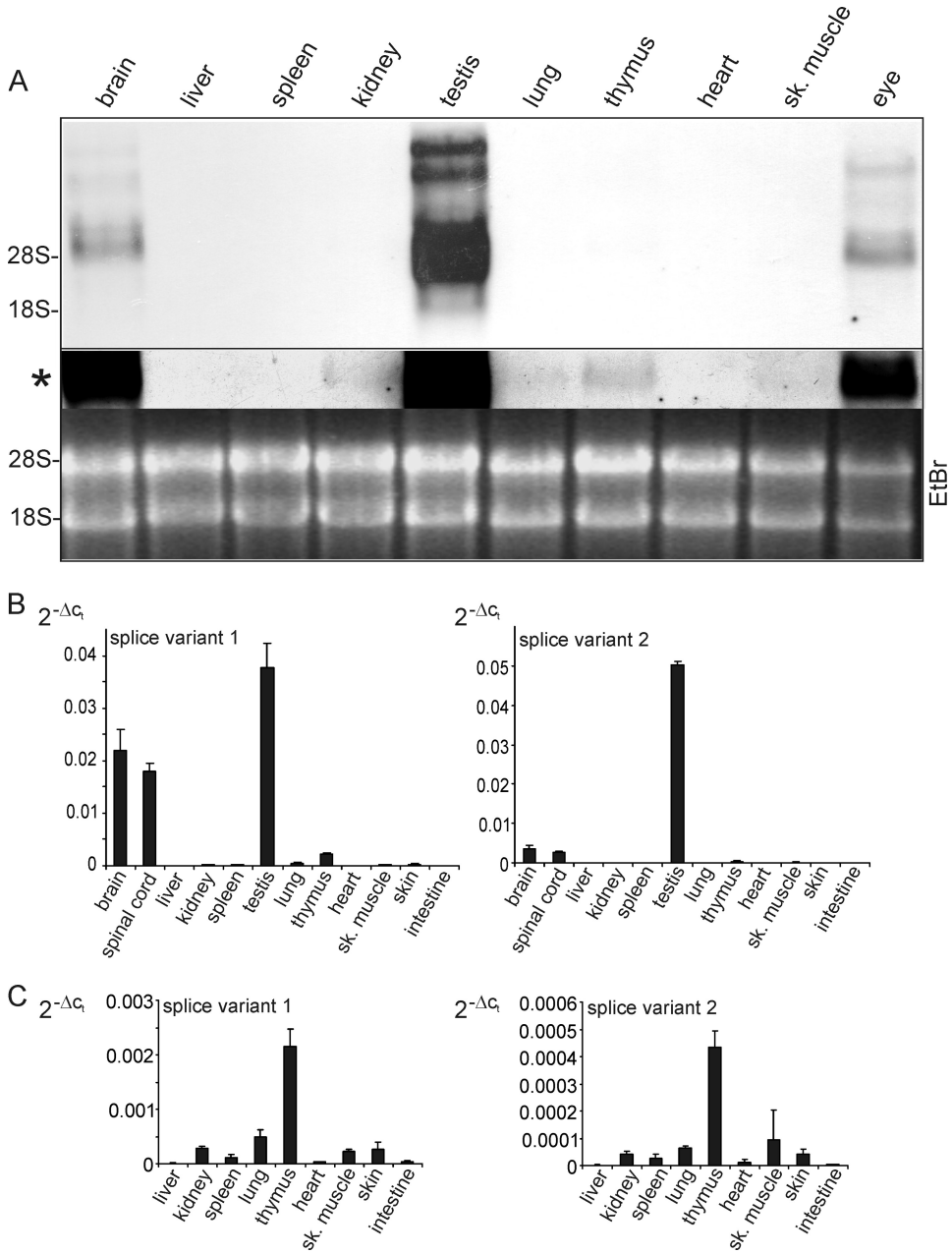

FIGURE 3. **Expression of NAAGS in different mouse tissues.** *A*, Northern blot analysis of NAAGS in different tissues of 10-week-old C57BL/6 mice. Northern blot membrane was hybridized to a full-length digoxigenin-labeled antisense cRNA probe, followed by chemiluminescence detection. High level expression was only found in brain and testis. Longer exposure times (*) showed also weak hybridization signals in thymus, lung, kidney, and skeletal muscle, in line with the real-time PCR data shown below. *B*, real-time RT-PCR of NAAGS expression in tissues of 10-week-old mice. *C*, upscaling of the panels shown in *B* revealed low expression of NAAG synthetase also in thymus, lung, skeletal muscle (sk. muscle), kidney, skin, spleen, and heart. No expression was found in the liver. The relative expression levels calculated by the $2^{-\Delta ct}$ method, normalized to ubiquitin C, are shown. The data shown are the mean ± S.E. ($n = 3$) of three independent experiments (using three independent RNA preparations from three different animals per tissue).

as housekeeping control. Data were analyzed by the $2^{-\Delta ct}$ method.

Plasmids—Mouse brain cDNA was synthesized from mouse brain total RNA by reverse transcription with superscript II reverse transcriptase (Invitrogen) using oligo(dT)-primer. NAAGS, NaDC3, and Nat8l cDNAs were amplified by PCR with Phusion™ DNA-polymerase (New England Biolabs, Frankfurt, Germany), using the oligonucleotides shown in supplemental Table S1. PCR products were digested with the appropriate restriction endonucleases and ligated into pFLAG (28), pEGFP-C1 (Clontech, Heidelberg, Germany), or pcDNA3 vector (Invitrogen) (see supplemental Table S1). All DNA constructs were confirmed by DNA sequencing. As controls the following plasmids were used: pFLAG-ME14 (encoding FLAG-tagged MacGAP (29) from hamster),[4] pDsRed, and pEGFP-C1 (Clontech) plasmids.

Western Blotting—SDS-PAGE and Western blotting using chemiluminescence detection was done as described (30). The following antibodies were used: mouse M2 anti-FLAG-epitope (Sigma), rabbit anti-green fluorescent protein (Abcam, Cambridge, United Kingdom), and peroxidase conjugated goat anti-mouse and anti-rabbit antisera (Dianova, Hamburg, Germany).

Cell Culture and Transfection—Mixed brain cultures were prepared from newborn mouse brains as described (31). After reaching confluency, microglia and oligodendrocytes were removed by incubating the culture flasks on an orbital shaker and the remaining astrocyte monolayer was trypsinized. Astrocytes were grown in DMEM medium containing 10% fetal calf serum (FCS), 2 mM L-glutamine, penicillin, and streptomycin. Astrocytes were transfected by electroporation using the Amaxa nucleofector kit (Amaxa, Cologne, Germany). CHO-K1 and HEK-293T cells were maintained in DMEM/Nut Mix F12 (1:1) with 10% FCS, 2 mM L-glutamine, penicillin, and streptomycin. HEK-293T cells were transfected using calcium phosphate. CHO-K1 cells were transfected using ExGen500 (Fermentas, St. Leon-Rot, Germany), according to the manufacturer's instruction. Human SH-SY5Y neuroblastoma cells were grown in DMEM/Nut Mix F12 (1:1) with 20% FCS, 1 mM L-glutamine, penicillin, and streptomycin.

Metabolic Labeling—For metabolic labeling, the medium was exchanged against 1 ml of fresh medium per 35-mm well, 16–20 h after transfection. Cells were metabolically labeled with [^{14}C]-glutamate (0.5 μCi/well), ^{14}C-protein hydrolysate

[4] M. Eckhardt, unpublished data.

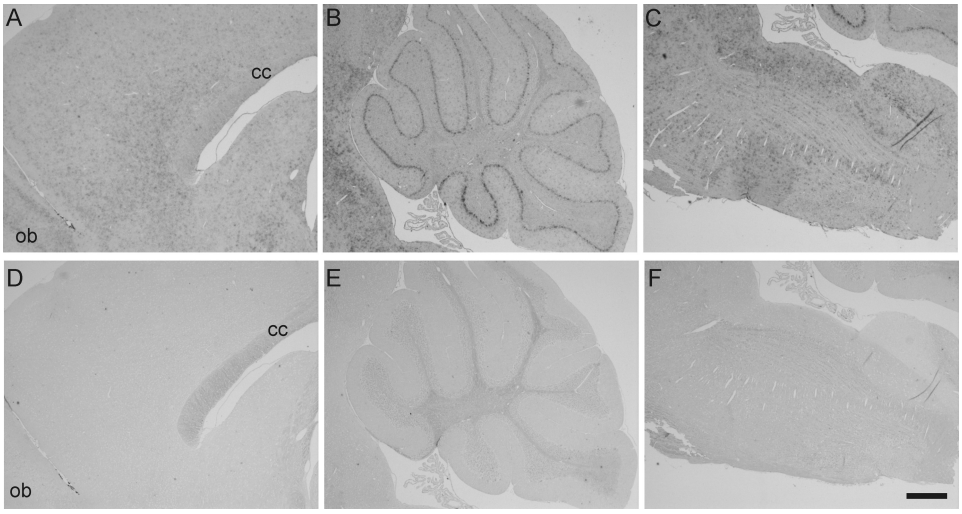

FIGURE 4. ***In situ* hybridization of mouse brain sections.** Paraffin sections of 10-week-old mouse brains were hybridized to digoxigenin-labeled cRNA NAAGS antisense (*A–C*) or sense probes (*D–F*). NAAGS expression was detectable in the neocortex (*A*), cerebellum (*B*), and stem brain (*C*). The higher signal intensities in the stem brain compared with forebrain is in line with the higher NAAG concentration in the former. *cc*, corpus callosum; *ob*, olfactory bulb. Scale bar, 500 μm.

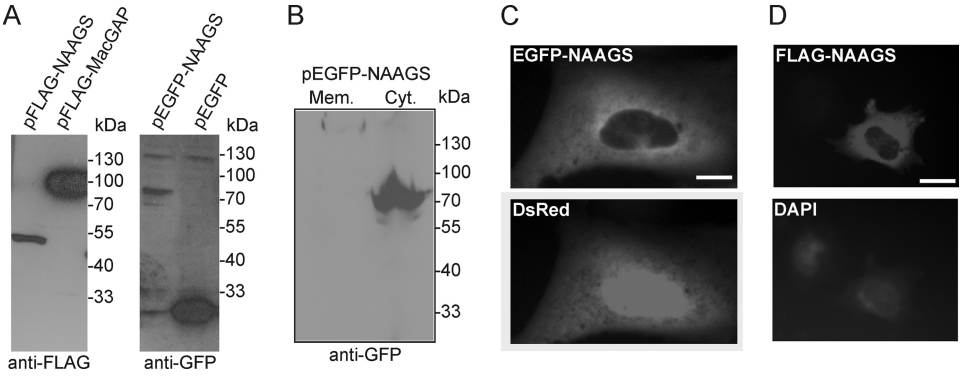

FIGURE 5. **Western blot and immunofluorescence analysis of NAAGS.** *A*, Western blot analysis of cell lysates from CHO-K1 cells transiently transfected with pFLAG-NAAGS, an irrelevant control plasmid (pFLAG-MacGAP), pEGFP-NAAGS, or empty pEGFP vector identified FLAG- and EGFP-tagged proteins of the expected molecular mass. *B*, subcellular fractionation of EGFP-NAAGS expressing CHO-K1 cells into total membrane fraction (*Mem.*) and cytosol (*Cyt.*), indicated cytosolic localization of NAAGS. *C*, fluorescence detection of EGFP-NAAGS coexpressed with DsRed. *D*, immunofluorescence detetction of FLAG-tagged NAAGS in transiently transfected CHO-K1 cells. Scale bars, 10 μm (*C*), 20 μm (*D*).

(GE Healthcare) (2 μCi/well), or [^{14}C]NAA (0.25 μCi/well) for 4 or 16 h. In some experiments, 10 mM NAA was added to the culture medium 1 h before starting the metabolic labeling. Cells were washed three times with phosphate-buffered salt solution (PBS) and scraped in 1 ml of ice-cold 90% methanol. Samples were centrifuged for 5 min at 10,000 $\times$ *g* and the peptide containing supernatant was dried in a speed vac concentrator. The dried extract was dissolved in water, and the pH was adjusted to 5–6 with sodium hydroxide, if necessary. To remove cations from the extract, the solution was passed through a cation exchange column (AG 50 W X8 resin; Bio-Rad, Munich, Germany), and the eluate fractions were dried in a speedvac concentrator. Dried samples were dissolved in 20 μl of 20% ethanol, containing 5 mM NAAG as internal standard, and applied onto silica gel 60 HPTLC plates (Merck, Darmstadt, Germany). Chromatograms were developed in one of the following solvent systems: (*a*) butanol/acetic acid/water (12:3:5) or (*b*) chloroform/methanol/acetic acid (9:1:5). Radioactive signals were visualized using Bioimager screens (Fujifilm, Düsseldorf, Germany). The unlabeled NAAG standard was detected by UV scanning at 215 nm.

Synthesis of ^{14}C-labeled NAA—Radioactive NAA was synthesized using [^{14}C]aspartate (GE Healthcare) and anhydrous acetic acid (Merck, Darmstadt, Germany). The reaction was started by adding 11.7 nmol of acetic acid anhydride to 2.7 nmol of [^{14}C]aspartate in 500 μl of water, and the reaction mixture was vigorously mixed for 30 min, until a phase separation was no longer visible. To remove any remaining cations, the reaction mixture was passed through a AG 50 W X8 cation exchange column (Bio-Rad).

NAA Transport Assay—NAA transport assays were done as described (23). Briefly, primary astrocytes or transfected CHO-K1 cells were washed twice with Locke's buffer (154 mM NaCl, 5.6 mM KCl, 3.6 mM $NaHCO_3$, 1.3 mM $CaCl_2$, 1 mM $MgCl_2$, 5 mM glucose, 10 mM HEPES, pH 7.4) and then incubated in Locke's buffer containing 4 μM [^{14}C]NAA for 40 min at 37 °C. Thereafter, cells were washed three-times with ice-cold Locke's buffer and lysed in 1% SDS. Radioactivity was determined by liquid scintillation counting.

In Situ Hybridization—Digoxigenin-labeled cRNA antisense and sense probes were transcribed from the pFLAG-NAAGS expression plasmid using respectively SP6- and T7-RNA polymerase, and digoxigenin-dNTP mix (Roche Molecular Diagnostics, Mannheim, Germany), according to the instructions of the manufacturer. Brain paraffin sections from 10-week-old C57BL/6 mice were hybridized to antisense and sense cRNA probes as described previously (32). Bound probes were visualized using anti-digoxigenin Ig-alkaline phosphatase conjugate and nitro blue tetrazolium chloride and 5-bromo-4-chloro-3-indolyl phosphate as substrate.

HPLC and ESI-MS—For HPLC/MS quantification of NAAG and NAA, cells were harvested 48 h after transfection. Cells were washed three times with PBS. Cell pellets from two 35-mm dishes were resuspended in 300 μl of ice-cold 90% methanol and sonicated. Protein precipitates were sedimented by centrifugation at 20,800 $\times$ *g* for 15 min at 4 °C. The protein pellet was used to measure protein concentration by the bicinchoninic acid assay (Bio-Rad). The peptide extract was dried under vacuum and dissolved in 200 μl of distilled water (overnight at room temperature). The solution was centrifuged at

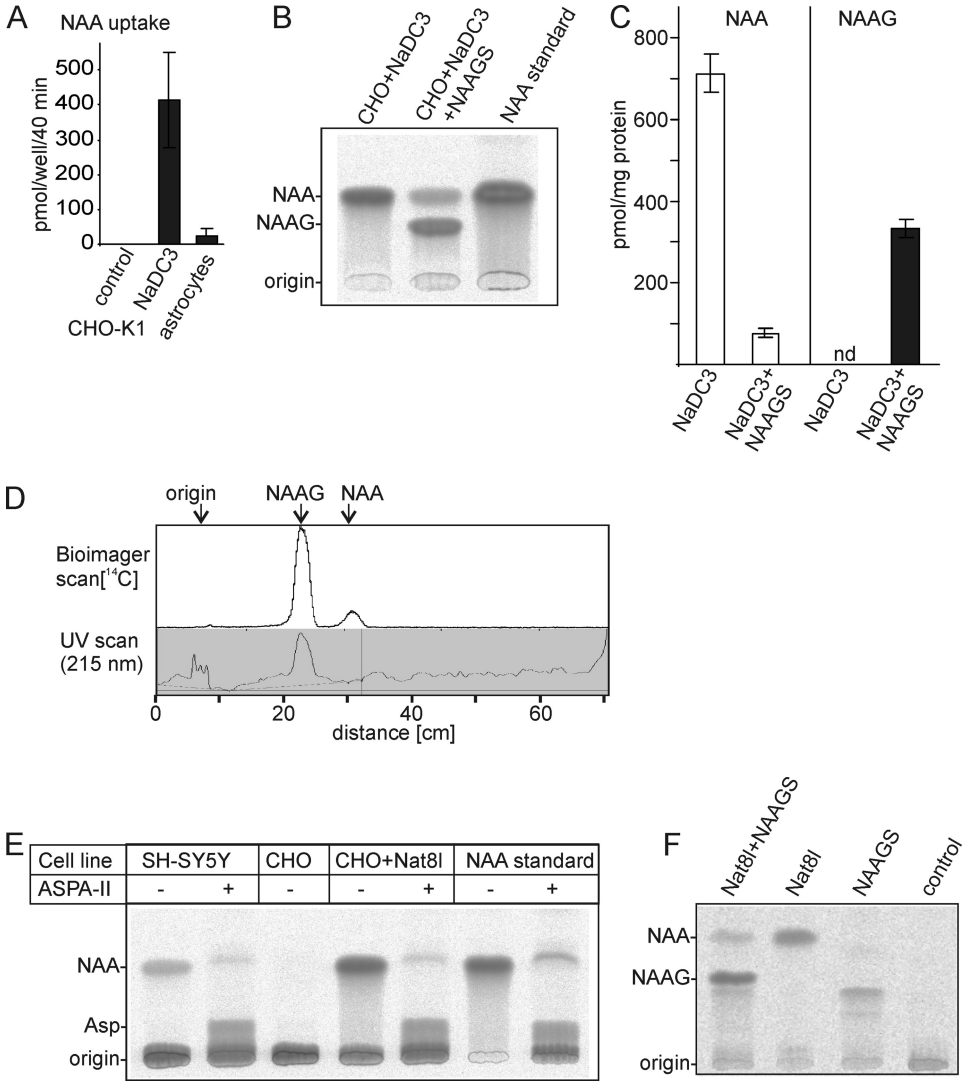

FIGURE 6. **NAAG synthesis by NAAGS.** *A*, NAA transport assay with untransfected CHO-K1 (control), CHO-K1 cells transiently transfected with a plasmid encoding the NAA transporter NaDC3, and primary astrocytes. *B*, thin layer chromatogram of peptide extracts from CHO-K1 cells transiently transfected with NaDC3 or NaDC3 together with NAAGS. Transfected cells were metabolically labeled with [^{14}C]NAA for 16 h. Methanolic peptide extracts were separated by TLC, and radioactivity was detected using a Bioimager screen. *C*, quantification of NAA and NAAG synthesized in CHO-K1 cells expressing NaDC3 or cells cotransfected with NaDC3 and NAAGS expression plasmids. *D*, representative Bioimager and UV (215 nm) scans of a thin layer chromatogram of a peptide extract from CHO-K1 cells coexpressing NAAGS and NaDC3 and metabolically labeled with [^{14}C]NAA. *E*, *in vitro* NAA synthase assay using [^{14}C]aspartate and acetyl-CoA. To confirm synthesis of NAA, aliquots of the reaction products were treated with ASPA-II. *F*, metabolic labeling with [^{14}C]glutamate of CHO-K1 cells transiently expressing Nat8l, Nat8l, and NAAGS, or NAAGS. Control cells were transfected with the plasmid pFLAG-ME14, encoding hamster MacGAP.

20,800 × *g* (20 min), and the supernatant was directly subjected to HPLC.

Samples were analyzed by a tandem LC/MS-spectroscopy method. For HPLC (HPLC 1200 series, Agilent Technologies, Santa Clara, CA) a column (organic acid resin 250 × 4 mm sphere image; CS-chromatography service GmbH, Langerwehe, Germany) of organic acid resin, PS-DVB with sulfonic acid changer, was used. The mobile phase consisted of 0.05% formic acid, and absorbance was detected at 214 nm. For equilibration, the column was washed with the mobile phase for 1 h with a flow rate of 1 ml/min. The flow rate for all analysis was 0.5 ml/min. The detection limit for the HPLC measurement of NAAG was 0.006 (HEK-293T cells) and 0.009 nmol/mg protein (CHO-K1 cells), respectively. The detection limit of NAA was 0.016 (HEK-293T cells) and 0.013 nmol/mg protein (CHO-K1 cells), respectively.

For ESI/MS (ESI-MS HCTultra, Bruker Daltonics, Billerica, MA) a negative ion mode with Auto/MS was used. Eluate fractions from the HPLC were directly injected. Nitrogen at a temperature of 350 °C was used as drying gas. The collision gas was a mixture of helium with 3% argon. The capillary voltage was set to 4,000 V.

RESULTS

Identification of a Putative Peptide Synthetase Expressed in the Mammalian Nervous System—Prokaryotes contain various peptide synthetases/amino acid ligases. In contrast, only few peptides in mammals are synthesized in a ribosome-independent manner, the most prominent example is the tripeptide glutathione. A comparison of known eukaryotic and prokaryotic peptide synthetases revealed significant sequence similarities. All of them contain a so called ATP-grasp domain (33). We hypothesized that the NAAG synthetase should be a brain-specifically expressed member of the ATP-grasp family of amino acid ligases. Therefore, BLAST searches were performed with known (eukaryotic and prokaryotic) dipeptide synthetases/amino acid ligases as queries. Identified sequences were then examined regarding their tissue specific expression pattern by examination of the EST databases. As NAAG is present in all vertebrates, but appear not to be absent in most invertebrates, the additional criterion was that the identified candidate genes have to be present in all vertebrates but not in invertebrates. A single gene, *Rimklb* ribosomal modification protein rimK-like family member B (GenBank™ accession number AA097693), fulfilled all these criteria. We renamed this gene NAAG synthetase (NAAGS). Orthologous sequences were found in all vertebrate genomes accessible in the ensemble genome database. Sequence alignment of NAAGS sequences from different vertebrates shows a high degree of similarity (Fig. 2*A*). The NAAGS sequence shows significant similarity to α-L-glutamate ligases (RimK family), and bacterial glutathione synthetases. RimK proteins add glutamate residues to the C terminus of the

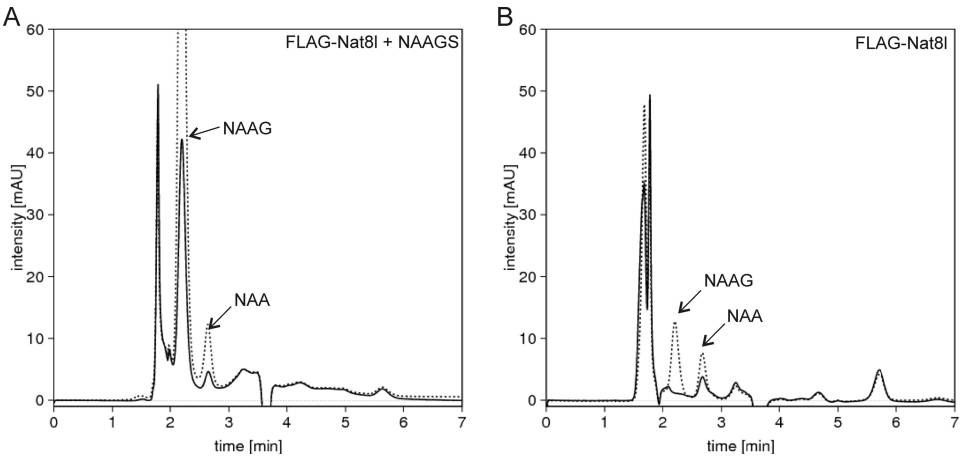

FIGURE 7. **HPLC detection and quantification of NAAG synthesis.** Representative HPLC spectra of methanolic extracts from transiently transfected cells are shown. *A*, HEK-293T cells cotransfected with plasmids encoding FLAG-Nat8l and NAAGS (*unbroken line*). The same peptide extract was reanalyzed after addition of NAAG and NAA as internal standards (*dotted line*). (B) CHO-K1 cells transfected with a plasmid encoding FLAG-Nat8l, analyzed in the absence (*unbroken line*) or presence (*dotted line*) of NAAG and NAA internal standards. NAAG and NAA concentrations were determined by integration of the HPLC peak areas. The combined data of all experiments are given in Table 1.

TABLE 1

NAAG synthesis in NAAGS-expressing cells

FLAG-tagged NAAGS was used in all experiments. Data shown are mean ± S.D. (n = 3) of three independent experiments.

Cell line	Transfected cDNAs	NAAG	NAA
		nmol/mg protein	*nmol/mg protein*
CHO-K1	NAAGS+NaDC3[a]	0.03 ± 0.01	0.17 ± 0.07
CHO-K1	NAAGS+Nat8l	0.07 ± 0.02	0.02 ± 0.00
CHO-K1	NAAGS	ND[b]	ND
CHO-K1	Nat8l	ND	0.12 ± 0.03
HEK-293T	NAAGS+NaDC3[a]	0.28 ± 0.08	1.16 ± 0.31
HEK-293T	NAAGS+Nat8l	0.39 ± 0.12	0.08 ± 0.02
HEK-293T	NAAGS	ND	ND
HEK-293T	Nat8l	ND	1.01 ± 0.16

[a] 10 mM NAA was added to the culture medium.
[b] ND, not detectable.

ribosomal protein S6, and other prokaryotic members of this family include *Methanococcus jannaschii* γ-F420–2:glutamate ligase and tetrahydromethanopterin:glutamate ligase (34). Sequence similarities are also found to bacterial D-alanine:D-alanine ligase and another recently identified mammalian dipeptide synthetase, *i.e.* carnosine synthetase (35) (see supplemental Fig. S1). Moreover, most residues of the ATP-grasp domain that have been shown to be involved in ATP binding in the D-alanine:D-alanine ligase from *Escherichia coli* (36) are conserved in NAAGS (see supplemental Fig. S1). The *Rimkla* gene, which is present in mammals but according to a database search not in other vertebrates, exhibits significant sequence similarity to NAAGS (Fig. 2*A*). Rimkla may also encode a NAAG synthetase. However, this possibility has not yet been tested experimentally.

Different mouse and human NAAGS mRNA variants, that potentially encode at least two different proteins (variants v1 and v2) that differ in their C terminus were found in the GenBank™ database (Fig. 2*B*). The presence of the two variants in mouse brain could be confirmed by 3′-rapid amplification of cDNA ends (data not shown).

Northern blot analysis demonstrated high level expression of NAAGS in the nervous system (Fig. 3*A*), though the highest expression level was found in testis. High expression levels of NAAGS in the eyes is in accordance with the significant amounts of NAAG in the retina (37). Relatively weak signals were observed in thymus, lung, kidney, and skeletal muscle (Fig. 3*B*). RT-PCR confirmed these data and revealed very low expression of NAAGS also in spleen, skin, and heart (Fig. 3*C*). NAAGS was undetectable in liver. The relative expression of the two splice variants v1 and v2 was comparable in all tissues, except for testis. The functional relevance of NAAGS expression in non-neuronal tissues is unclear, as it is not known whether the NAA synthase Nat8l (38) is also expressed in these tissues.

In situ hybridization of brain paraffin sections using digoxigenin-labeled NAAGS antisense cRNA probes showed expression of NAAGS in neurons of various brain regions, including the neocortex (Fig. 4*A*), with relatively high expression levels in the midbrain (Fig. 4*B*), the gray matter of the brainstem (Fig. 4*C*), and Purkinje cells in the cerebellum (Fig. 4*B*). The strong expression in the brainstem and midbrain is in line with the high NAAG concentration in neurons of this area (6).

pFLAG-NAAGS and pEGFP-NAAGS plasmids encoding NAAGS with N-terminal FLAG or EGFP-tag were generated. Western blot analysis of FLAG- and EGFP-tagged variants of NAAGS identified proteins of about 45 and 70 kDa, respectively, in cell lysates of transiently transfected CHO-K1 cells (Fig. 5, *A* and *B*), in agreement with the predicted molecular mass of the proteins. Fluorescence detection of the EGFP- and FLAG-tagged NAAGS suggested cytosolic expression of the protein (Fig. 5, *C* and *D*), which was confirmed by subcellular fractionation (Fig. 5*B*). The following experiments were performed using FLAG epitope-tagged NAAGS.

NAAG Synthesis in NAAGS-expressing Cells—No *in vitro* NAAG synthetase assay has been described. Therefore, to test our hypothesis that the NAAGS gene encodes NAAG synthetase, we initially expressed NAAGS (variant v1) in primary astrocytes, which are known to express the NAA transporter NaDC3 (39). Transfected cells were incubated for 4 h with [^{14}C]glutamate (in the absence or presence of unlabeled 10 mM NAA in the culture medium). TLC analysis of peptide extracts from NAAGS-expressing astrocytes revealed a radioactive product comigrating with NAAG standard that was absent from control cells (data not shown).

Because uptake of NAA by astrocytes was relatively low, and furthermore, to address the question whether NAAGS expression was sufficient to induce NAAG synthesis in a cell line with no intrinsic NAA/NAAG metabolizing enzyme activities, further tests were performed in CHO-K1 cells. NAA uptake was significantly increased in CHO-K1 cells transiently expressing the NaDC3 transporter, when compared with primary astro-

cytes (Fig. 6*A*). CHO-K1 cells expressing NaDC3 or NAAGS alone or in combination were metabolically labeled by addition of [^{14}C]NAA to the culture medium for 16 h. A methanolic peptide extract of the cells was subjected to TLC analysis (Fig. 6, *B* and *C*). A radioactive product comigrating with NAAG standard (added as internal standard and detected by UV scanning; see Fig. 6*D*) was detectable only when NAAGS was coexpressed with NaDC3.

The NAAG precursor NAA is synthesized by the NAA synthase (*N*-acetyltransferase Nat8l; Ref. 38). As shown in Fig. 6*E*, NAA synthase activity is absent from untransfected CHO-K1 cells, but can be detected in cell lysates from CHO-K1 cells expressing Nat8l. To confirm identity of the reaction product, reaction mixtures were treated with aspartoacylase-II, which specifically hydrolyzes NAA (Fig. 6*E*, +*ASPA-II*). We transiently coexpressed NAAGS and NAA synthase (Nat8l) in CHO-K1 cells and metabolically labeled them with [^{14}C]glutamate. In cells expressing Nat8l, NAA but no NAAG was synthesized (Fig. 6*F*). In cells coexpressing Nat8l and NAAGS, NAAG was synthesized. In addition, minor radioactive products could be detected that were absent from cells transfected with a control vector. However, the same reaction products were visible in cells transfected only with NAAGS cDNA, indicating that they do not contain NAA. Accordingly, these products were not observed when cells were metabolically labeled with [^{14}C]NAA (Fig. 6*B*). Because of the low abundance of these products, it was not yet possible to identify them.

The expression of the NAAGS splice variant 2 after transient transfection was very low, and we were unable to detect any reaction products of this variant by metabolic labeling or mass spectrometry of peptide extracts (data not shown). Thus, it remains unknown whether NAAGS variant v2 encodes an active NAAG synthetase. It may be

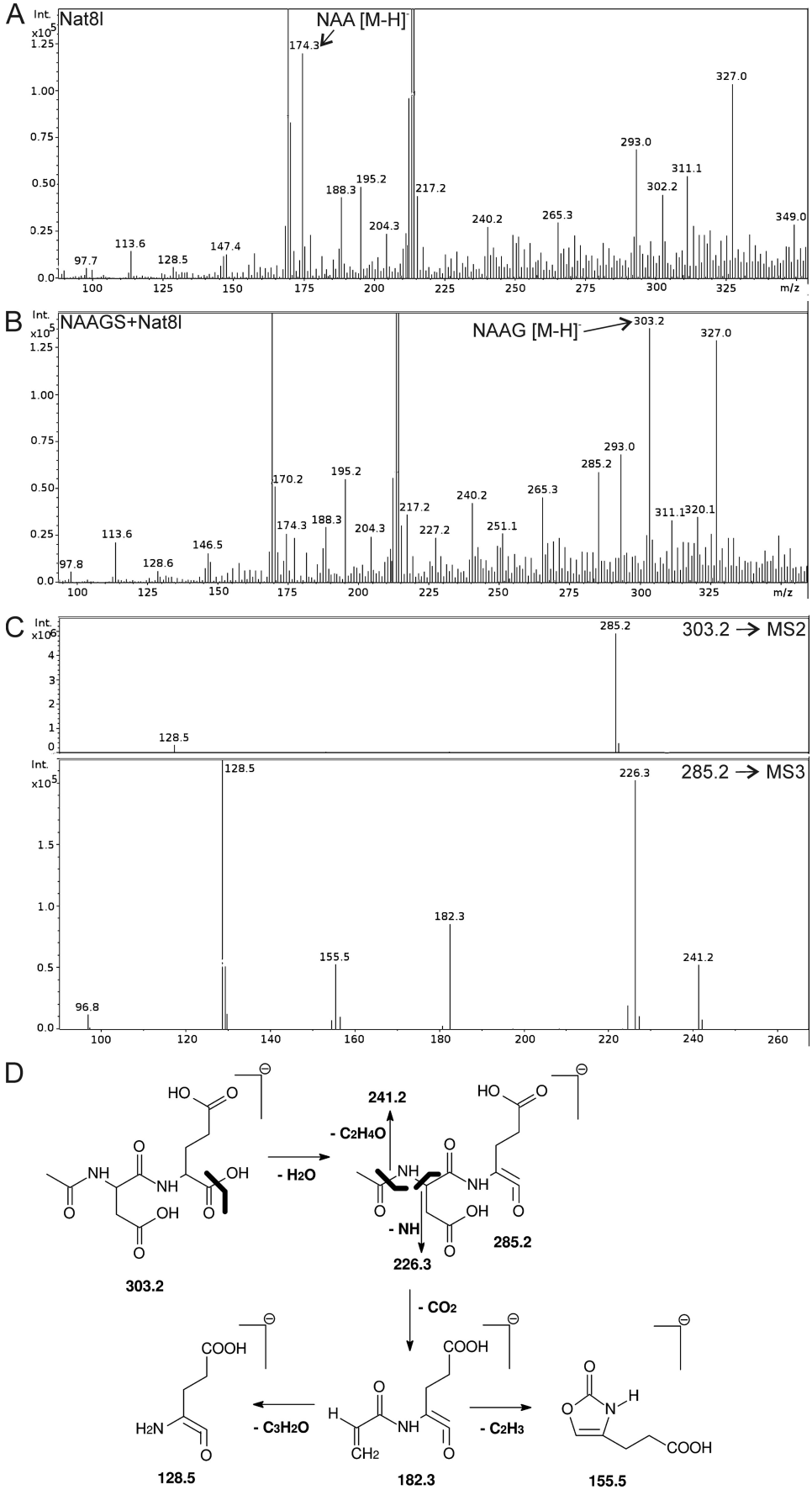

that the protein or its mRNA are very unstable. The latter possibility is supported by the fact that the size of the major NAAGS mRNA as detected by Northern blotting corresponds to the predicted size of the v1 variant (4.7 kb), whereas no signal corresponding to the expected size of the v2 variant (<3 kb) was detectable in brain (see Fig. 3*A*).

Taken together, the above data show that in the presence of NAA, expression of NAAGS (variant v1) is necessary and sufficient to induce synthesize of a dipeptide, comigrating with NAAG, using NAA as substrate, strongly suggesting that NAAGS is an *N*-acetylaspartylglutamate synthetase.

HPLC/MS Detection of NAAG in NAAGS-expressing Cell Lines—To confirm the structural identity of the NAAGS reaction product, we repeated the assays using unlabeled NAA and analyzed peptide extracts of transfected cells by HPLC and mass spectrometry. CHO-K1 or HEK-293T cells were transiently transfected with NAAGS and the NaDC3 transporter or Nat8l, and incubated for 16 h with or without 10 mM NAA added to the culture medium. The peptide containing methanol extract was subjected to HPLC and NAAG and NAA were detected by UV(214 nm) measurement using authentic NAAG and NAA as references. The eluate was further subjected to mass spectrometry using an ion-trap ESI-MS. Only in cells transfected with NAAGS together with Nat8l or NaDC3 (and then in the presence of NAA in the culture medium) did we observe a reaction product comigrating with the NAAG standard by HPLC (Fig. 7*A*; Table 1). In cells expressing only Nat8l, NAA but no NAAG was detectable (Fig. 7*B*).

The eluate fractions of the HPLC were further examined by ESI-MS (in negative ion mode). The expected mass peak of $m/z = 303.2$ $[M\text{-}H]^-$ for NAAG was absent from cells expressing only Nat8l (Fig. 8*A*). However, a mass peak at $m/z = 174.3$ was in line with the presence of NAA (which was further confirmed by tandem-MS; data not shown). In accordance with the metabolic labeling experiments shown above, the NAA mass peak declined in cells coexpressing Nat8l and NAAGS, whereas a mass peak of $m/z = 303.2$ $[M\text{-}H]^-$ was in accordance with the presence of NAAG (Fig. 8*B*). Tandem MS (MS2 and MS3) of this ion generated a fragmentation pattern (Fig. 8*C*) that was in agreement with the NAAG structure (Fig. 8*D*) and identical to the fragmentation pattern of authentic NAAG standard (data not shown).

DISCUSSION

Using a bioinformatic approach, we identified a new member of the ATP-grasp domain family that is strongly expressed in the nervous system. A similar approach recently led to the identification of the NAA synthase (38). Thus, all enzymes directly involved in the metabolism of NAAG (see Fig. 1) have now been characterized at the molecular level.

The following arguments clearly indicate that the newly identified gene encodes a NAAG synthetase: 1) NAAG was produced in all cell types tested, when they expressed NAAGS; 2) NAAG synthesis strictly depended on the presence of NAA; and 3) ESI-MS tandem mass spectrometry of the mass peak of $m/z = 303.2$ generated the expected fragment ions, demonstrating the presence of NAAG in cell lines expressing NAAGS in combination with NAA synthase or NaDC3 transporter. In addition, the expression pattern as determined by Northern blotting, RT-PCR, and *in situ* hybridization was in accordance with the tissue-specific distribution of NAAG reported in the literature. Although we observed high expression level of NAAGS in testis, presence of NAAG in this tissue has, to our knowledge, not been described. Probably, low NAA levels may limit NAAG synthesis in testis, as we found only very low or no expression of the NAA synthase Nat8l in mouse testis samples by quantitative real-time RT-PCR.[5]

Two glutamate carboxypeptidases (GCP-II and GCP-III) capable of hydrolyzing NAAG have been identified (40, 41). In rat brain, GCP-II is expressed in almost all astrocytes (42). The distribution of NAAGS expression was to some extent comparable to that of GCP-II, reported by Luthi-Carter *et al.* (43). Both, NAAGS and GCP-II show higher expression levels in the midbrain and brainstem compared with the neocortex. Furthermore, the relatively intense NAAGS *in situ*-hybridization signal found in the Purkinje cell layer of the cerebellum correlates with the strong expression signals in Bergmann glia cells adjacent to the Purkinje cells (42, 43).

There is no *in vitro* NAAGS enzyme assay available. Initial experiments to demonstrate *in vitro* enzyme activity in cell lysates from NAAGS-overexpressing cells were also unsuccessful.[6] Furthermore, attempts to demonstrate its *in vitro* activity using bacterial expressed NAAGS protein failed, because the recombinant protein was completely insoluble and entirely present in inclusion bodies.[6] Therefore, we cannot formally rule out the possibility that additional specific co-factors are needed for NAAG synthesis. However, this appear to be unlikely as these cofactors would also be present in cell lines like CHO-K1 or HEK-293T, that *per se* do not contain the enzymatic machinery of NAAG metabolism.

NAAG is released in a calcium-dependent manner from synaptic terminals upon depolarization (for review see Ref. 1), suggesting its presence in synaptic vesicles. Our data show that NAAGS is localized to the cytosol of transiently transfected CHO-K1 cells. Thus, there must be a (vesicular) peptide transporter responsible for the transport of NAAG into synaptic vesicles. Such a transporter has to our knowledge not been identified yet. Formally, however, we cannot exclude the possibility that the subcellular localization of NAAGS in neurons differs from that in transiently transfected CHO-K1 cells.

When NAA levels in cells expressing NAA synthase Nat8l alone are compared with cells coexpressing NAA synthase and

[5] L. Wang-Eckhardt and M. Eckhardt, unpublished observation.
[6] J. Lodder and M. Eckhardt, unpublished observation.

FIGURE 8. **ESI-MS/MS detection of NAAG.** Methanolic peptide extracts from transiently transfected cells were subjected to HPLC (as shown in Fig. 7), and eluate fractions containing NAAG were directly analyzed by ESI-MS in the negative ion mode. *A*, ESI-MS mass spectrum of peptide extract from HEK-293T cells expressing only Nat8l. The mass peak at $m/z = 174.3$, which was not present in mock-transfected controls (data not shown), corresponds to NAA $[M\text{-}H]^-$, which was also confirmed by tandem MS fragmentation (data not shown). *B*, mass spectrum of peptide extract from cells coexpressing NAAGS and Nat8l revealed a mass peak with $m/z = 303.2$, which was absent from control cells (*A*), and corresponds to the mass of NAAG $[M\text{-}H]^-$. *C*, MS/MS (MS2) and MS3 fragmentation generated ion fragments $[M\text{-}H]^-$ that were in agreement with the presence of NAAG (see fragmentation scheme in *D*).

NAAG synthetase, it is obvious that the steady state level of NAA in the latter was strongly reduced, suggesting a very efficient channeling of synthesized NAA to NAAG synthesis. The NAA synthase Nat8l is a membrane-bound enzyme of the ER (38), whereas NAAGS is a soluble protein in the cytosol. The membrane topology of Nat8l, which contains a single transmembrane domain, has not been determined yet, but one should expect that the carboxyl-terminal catalytic domain is localized to the cytosolic side of the ER membrane. It would be interesting to examine whether these two functionally interacting enzymes also interact physically.

While metabolic labeling of NAAGS-expressing cells with [^{14}C]NAA generated a single radioactive product that could be identified as NAAG, labeling with [^{14}C]glutamate in addition allowed detection of minor products, beside the main product, NAAG. These products were generated independent of the presence of NAA. Probably, NAAGS has a broader substrate specificity and may to some extent accept other amino acids or biogenic amines. In line with this, other dipeptide synthetases show a relatively broad substrate specificity. For example, carnosine synthetase uses both, beta-alanine and GABA to synthesize carnosine and homocarnosine, respectively (44). Moreover, using purified carnosine synthetase, Drozak *et al.* (35) could show that the enzyme, which also belongs to the ATP-grasp domain family, accepts different amino acids or amines as the second substrate. The physiological relevance of the additional NAAGS products, if produced at all *in vivo*, remains to be determined.

Synthesis of NAA and NAAG in human neuroblastoma cells may in part be regulated by protein kinase C and A activity (45). Potential protein kinase C and A phosphorylation sites are present in the NAAGS sequence, though it is currently not known, whether NAAGS is a substrate of one these kinases. The further characterization of NAAG synthetase described here, and the generation of NAAGS-deficient mice, which will be available in the future, will probably improve our understanding of the physiological and pathophysiological role of this abundant neuropeptide.

REFERENCES

1. Neale, J. H., Bzdega, T., and Wroblewska, B. (2000) *J. Neurochem.* **75,** 443–452
2. Baslow, M. H. (2000) *J. Neurochem.* **75,** 453–459
3. Coyle, J. T. (1997) *Neurobiol. Dis.* **4,** 231–238
4. Curatolo, A., D'Arcangelo, P., Lino, A., and Brancati, A. (1965) *J. Neurochem.* **12,** 339–342
5. Miyamoto, E., Kakimoto, Y., and Sano, I. (1966) *J. Neurochem.* **13,** 999–1003
6. Koller, K. J., Zaczek, R., and Coyle, J. T. (1984) *J. Neurochem.* **43,** 1136–1142
7. Cangro, C. B., Namboodiri, M. A., Sklar, L. A., Corigliano-Murphy, A., and Neale, J. H. (1987) *J. Neurochem.* **49,** 1579–1588
8. Moffett, J. R., Ross, B., Arun, P., Madhavarao, C. N., and Namboodiri, A. M. (2007) *Prog. Neurobiol.* **81,** 89–131
9. Huang, W., Wang, H., Kekuda, R., Fei, Y. J., Friedrich, A., Wang, J., Conway, S. J., Cameron, R. S., Leibach, F. H., and Ganapathy, V. (2000) *J. Pharmacol. Exp. Ther.* **295,** 392–403
10. Burri, R., Steffen, C., and Herschkowitz, N. (1991) *Dev. Neurosci.* **13,** 403–411
11. Namboodiri, A. M., Peethambaran, A., Mathew, R., Sambhu, P. A., Hershfield, J., Moffett, J. R., and Madhavarao, C. N. (2006) *Mol. Cell. Endocrinol.* **252,** 216–223
12. Burlina, A. P., Ferrari, V., Divry, P., Gradowska, W., Jakobs, C., Bennett, M. J., Sewell, A. C., Dionisi-Vici, C., and Burlina, A. B. (1999) *Eur. J. Pediatr.* **158,** 406–409
13. Kumar, S., Mattan, N. S., and de Vellis, J. (2006) *Ment. Retard. Dev. Disabil. Res. Rev.* **12,** 157–165
14. Lea, P. M., 4th, Wroblewska, B., Sarvey, J. M., and Neale, J. H. (2001) *J. Neurophysiol.* **85,** 1097–1106
15. Huang, L., Rowan, M. J., and Anwyl, R. (1999) *Eur. J. Pharmacol.* **366,** 151–158
16. Neale, J. H., Olszewski, R. T., Gehl, L. M., Wroblewska, B., and Bzdega, T. (2005) *Trends Pharmacol.* **26,** 477–484
17. Tsai , S. J. (2005) *Central Med. Sci. Monit.* **11,** 39–45
18. Chopra, M., Yao, Y., Blake, T. J., Hampson, D. R., and Johnson, E. C. (2009) *J. Pharmacol. Exp. Ther.* **330,** 212–219
19. Wolf, N. I., Willemsen, M. A., Engelke, U. F., van der Knaap, M. S., Pouwels, P. J., Harting, I., Zschocke, J., Sistermans, E. A., Rating, D., and Wevers, R. A. (2004) *Neurology* **62,** 1503–1508
20. Sartori, S., Burlina, A. B., Salviati, L., Trevisson, E., Toldo, I., Laverda, A. M., and Burlina, A. P. (2008) *Eur. J. Paediatr. Neurol.* **12,** 348–350
21. Williamson, L. C., and Neale, J. H. (1988) *Brain Res.* **475,** 151–155
22. Urazaev, A. K., Grossfeld, R. M., Fletcher, P. L., Speno, H., Gafurov, B. S., Buttram, J. G., and Lieberman, E. M. (2001) *Neuroscience* **106,** 237–247
23. Gehl, L. M., Saab, O. H., Bzdega, T., Wroblewska, B., and Neale, J. H. (2004) *J. Neurochem.* **90,** 989–997
24. Arun, P., Madhavarao, C. N., Hershfield, J. R., Moffett, J. R., and Namboodiri, M. A. (2004) *Neuroreport* **15,** 1167–1170
25. Wallace, I. M., O'Sullivan, O., Higgins, D. G., and Notredame, C. (2006) *Nucleic Acids Res.* **34,** 1692–1699
26. Eckhardt, M., Mühlenhoff, M., Bethe, A., and Gerardy-Schahn, R. (1996) *Proc. Natl. Acad. Sci. U.S.A.* **93,** 7572–7576
27. Becker, I., Wang-Eckhardt, L., Yaghootfam, A., Gieselmann, V., and Eckhardt, M. (2008) *Histochem. Cell Biol.* **129,** 233–241
28. Münster, A. K., Eckhardt, M., Potvin, B., Mühlenhoff, M., Stanley, P., and Gerardy-Schahn, R. (1998) *Proc. Natl. Acad. Sci. U.S.A.* **95,** 9140–9145
29. Li, X., Liu, Q., Liu, S., Zhang, J., and Zhang, Y. (2008) *Acta Biochim. Biophys. Sin. (Shanghai)* **40,** 855–863
30. Eckhardt, M., Barth, H., Blöcker, D., and Aktories, K. (2000) *J. Biol. Chem.* **275,** 2328–2334
31. Fewou, S. N., Ramakrishnan, H., Büssow, H., Gieselmann, V., and Eckhardt, M. (2007) *J. Biol. Chem.* **282,** 16700–16711
32. Fewou, S. N., Büssow, H., Schaeren-Wiemers, N., Vanier, M. T., Macklin, W. B., Gieselmann, V., and Eckhardt, M. (2005) *J. Neurochem.* **94,** 469–481
33. Galperin, M. Y., and Koonin, E. V. (1997) *Protein Sci.* **6,** 2639–2643
34. Li, H., Xu, H., Graham, D. E., and White, R. H. (2003) *Proc. Natl. Acad. Sci. U.S.A.* **100,** 9785–9790
35. Drozak, J., Veiga-da-Cunha, M., Vertommen, D., Stroobant, V., and van Schaftingen, E. (2010) *J. Biol. Chem.* **285,** 9346–9356
36. Fan, C., Moews, P. C., Shi, Y., Walsh, C. T., and Knox, J. R. (1995) *Proc. Natl. Acad. Sci. U.S.A.* **92,** 1172–1176
37. Anderson, K. J., Borja, M. A., Cotman, C. W., Moffett, J. R., Namboodiri, M. A., and Neale, J. H. (1987) *Brain Res.* **411,** 172–177
38. Wiame, E., Tyteca, D., Pierrot, N., Collard, F., Amyere, M., Noel, G., Desmedt, J., Nassogne, M. C., Vikkula, M., Octave, J. N., Vincent, M. F., Courtoy, P. J., Boltshauser, E., and van Schaftingen, E. (2010) *Biochem. J.* **425,** 127–136
39. Fujita, T., Katsukawa, H., Yodoya, E., Wada, M., Shimada, A., Okada, N., Yamamoto, A., and Ganapathy, V. (2005) *J. Neurochem.* **93,** 706–714
40. Bzdega, T., Turi, T., Wroblewska, B., She, D., Chung, H. S., Kim, H., and Neale, J. H. (1997) *J. Neurochem.* **69,** 2270–2277
41. Bzdega, T., Crowe, S. L., Ramadan, E. R., Sciarretta, K. H., Olszewski, R. T., Ojeifo, O. A., Rafalski, V. A., Wroblewska, B., and Neale, J. H. (2004) *J. Neurochem.* **89,** 627–635
42. Berger, U. V., Luthi-Carter, R., Passani, L. A., Elkabes, S., Black, I., Konradi, C., and Coyle, J. T. (1999) *J. Comp. Neurol.* **415,** 52–64
43. Luthi-Carter, R., Berger, U. V., Barczak, A. K., Enna, M., and Coyle, J. T. (1998) *Proc. Natl. Acad. Sci.* U.S.A. **95,** 3215–3220
44. Horinishi, H., Grillo, M., and Margolis, F. L. (1978) *J. Neurochem.* **31,** 909–919
45. Arun, P., Madhavarao, C. N., Moffett, J. R., and Namboodiri, M. A. (2006) *J. Neurochem.* **98,** 2034–2042